34th Annual International Conference of the IEEE EMBS
San Diego, California USA, 28 August - 1 September, 2012

Virtual Colon Tagging for Electronic Cleansing in Dual-energy Fecal-tagging CT Colonography*

Wenli Cai, Se Hyung Kim, June-Goo Lee, and Hiroyuki Yoshida, *Member, IEEE*

***Abstract*— Partial volume effect (PVE) and tagging inhomogeneity are two major causes of artifacts in electronic cleansing (EC) for fecal-tagging CT colonography (CTC). Our purpose was to develop a novel method called "virtual tagging" for electronic cleansing in dual-energy fecal-tagging CTC. A three-material decomposition scheme was first applied in dual-energy CTC to decompose each voxel into a mixture of air, soft tissue, and iodine-tagged fecal material. The entire colonic lumen was then marked by virtually tagging the mixture portion of luminal air at each voxel. As a result, colon lumen including air and tagged materials was segmented and subtracted by their high values in virtually tagged images. Our virtual tagging scheme provides a cleansed colon that is free from artifacts caused by the PVE at air-tagging mixture and inhomogeneous tagging.**

I. Introduction

Fecal tagging in CT colonography (CTC) is a promising method for differentiating residual feces from colonic soft-tissue structures in CTC images by 'marking' fecal materials using an oral contrast agent (iodine or barium). *Electronic cleansing* (EC) of the colon is a promising technique for removing the tagged fecal materials in CTC images to 'virtually' cleanse the colon after image acquisition.

Partial volume effect (PVE) is a mixture of CT numbers (attenuation values) of multiple materials in a single voxel. A typical mixture in CTC caused by PVE is *air-tagging* boundary (AT-boundary), which is a mixture of air and tagged fecal residues. AT-boundary represents a wide spectrum of CT values typically ranging from -800 HU to 600 HU. This air-tagging mixture not only have CT values significantly overlapping with that of soft-tissue structures, but also may have gradient values that are close to those of soft-tissue structures [1]. Most existing EC methods tend to use gradient-based approaches to detect an AT-boundary. However, such methods tend to erroneously remove a part or the entire thin soft-tissue structure (colonic folds or wall) that is sandwiched between tagged region and air lumen, which we call *air-tissue-tagging* layer (ATT-layer), or preserve a part or the entire AT-boundary, especially when the tagging level is low or at the junctions at which AT-boundary hits the colonic wall. The former causes the degradation (such as a false fistula) of the thin colonic wall and folds, and the latter creates pseudo soft-tissue structures, as demonstrated in Fig. 1. To address these artifacts, advanced methods, such as the local roughness analysis method [1] and the statistical classification method [2], have been proposed. However, these solutions are heuristic and incomplete because PVE is an ill-posed condition in single-energy CTC images, which cannot be completely solved as far as the conventional single-energy CT images are used.

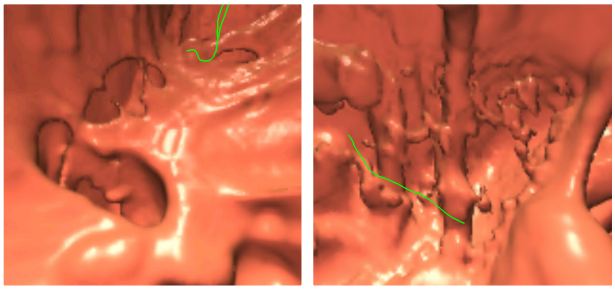

(a) (b)

Fig. 1. Demonstrations of EC artifacts. (a) False-fistula caused by the over-cleansed air-tissue-tagging layer (ATT-layer). (b) Pseudo-soft-tissue structures caused by the uncleansed air-tagging mixture at the air-tagging boundary (AT-boundary).

Dual-energy CT (DE-CT), which recently became widely available in clinical practice thanks to the technical advances, such as dual-source and fast kVp switching, provides a theoretical means of solving the material mixture by an analysis of two attenuation values acquired simultaneously at two photon energies (such as 80 kVp and 140 kVp) [3, 4]. This material decomposition ability in DE-CT works especially well in materials that have a *K*-edge energy close to the peak energy of the diagnostic CT imaging [5, 6], such as iodine. Iodine is a commonly used orally administered contrast agent in fecal-tagging CTC [7], and it is generally known to have strong enhancement at a low photon energy. Applying DE-CT to fecal-tagging CTC image acquisition, denoted as *DE-CTC*, provides a means of identifying the material mixtures, and thus can fully address these artifacts in EC [8-10].

In this study, we developed a dual-energy EC (DE-EC) scheme for minimizing the EC artifacts caused by the PVE and tagging inhomogeneity. This approach employed a novel method called "virtual tagging" (VT) that virtually marks the entire colonic lumen by tagging the luminal air and its mixture at each voxel in DE-CTC images to distinguish air-tagging mixtures from those of soft-tissues structures. As a result, colonic lumen, including air and tagged materials, was

*Research supported partly by Research Scholar Grant RSG-11-076-01-CCE from the American Cancer Society, and by Grant Numbers R01CA095279, R01CA131718, and R03CA156664 from National Cancer Institute (NCI).

Wenli Cai is with the Department of Radiology, Massachusetts General Hospital and Harvard Medical School, Boston, MA 02114 USA (phone: 617-726-0515; fax: 617-724-6130; e-mail: cai.wenli@mgh.harvard.edu).

Se Hyung Kim is with the Department of Radiology, Seoul National University Hospital College of Medicine, Seoul 110-744, Korea (e-mail: shkim@radcom.snu.ac.kr).

June-Goo Lee and Hiroyuki Yoshida are with the Department of Radiology, Massachusetts General Hospital and Harvard Medical School, Boston, MA 02114 USA (e-mail: lee.june, yoshida.hiro@mgh.harvard.edu).

segmented and subtracted by their high VT values. Our DE-EC scheme may provide a cleansed colon that is free from artifacts caused by the PVE at air-tagging boundary.

II. METHODS

A. Three-material Decomposition in DE-CTC

In DE-CTC scanning, there are two CT values at a point $\boldsymbol{x}$, $u^L(\boldsymbol{x})$ and $u^H(\boldsymbol{x})$, which are the CT values at low (80 kVp) and high (140 kVp) energies, respectively. Suppose that the material at each voxel, $m(\boldsymbol{x})$, is a mixture of three base materials m_1, m_2, and m_3:

$$m(\boldsymbol{x}) = p_1(\boldsymbol{x})m_1 + p_2(\boldsymbol{x})m_2 + p_3(\boldsymbol{x})m_3\ , \tag{1}$$

where p_i is the mixture ratio of material m_i, and it satisfies $p_1 + p_2 + p_3 = 1$.

Thus, the CT value of the voxel at low and high energy can be represented by Equation (2):

$$\begin{pmatrix} u^L(\boldsymbol{x}) \\ u^H(\boldsymbol{x}) \end{pmatrix} = p_1(\boldsymbol{x}) \begin{pmatrix} u^L_{m_1} \\ u^H_{m_1} \end{pmatrix} + p_2(\boldsymbol{x}) \begin{pmatrix} u^L_{m_2} \\ u^H_{m_2} \end{pmatrix} + p_3(\boldsymbol{x}) \begin{pmatrix} u^L_{m_3} \\ u^H_{m_3} \end{pmatrix}, \tag{2}$$

where $(u^L_{m_i}, u^H_{m_i})$ are two CT values of material m_i at low (80 kVp) and high (140 kVp) energies, respectively.

Consider a triangle $m_1m_2m_3$ defined by three vertices $m_1(u^L_{m_1}, u^H_{m_1})$, $m_2(u^L_{m_2}, u^H_{m_2})$, and $m_3(u^L_{m_3}, u^H_{m_3})$. The mixture ratios p_1, p_2 and p_3 in Equation (2) are the barycentric coordinates of this triangle that can be calculated in terms of the triangle areas A_1, A_2, and A_3, as illustrated in Fig. 2.

Therefore, we may form an equivalent linear system

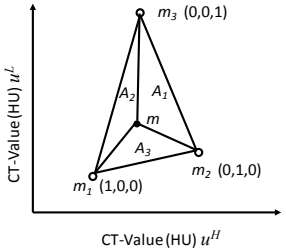

Fig. 2. A triangle is given by three points $m_1m_2m_3$. The barycentric coordinates of a point m with respect to the triangle $m_1m_2m_3$ are defined in terms of ratios of triangle areas: A_1, A_2, and A_3.

based on Equations (1) and (2):

$$\begin{pmatrix} u^L_{m_1} & u^L_{m_2} & u^L_{m_3} \\ u^H_{m_1} & u^H_{m_2} & u^H_{m_3} \\ 1 & 1 & 1 \end{pmatrix} \begin{pmatrix} p_1(\boldsymbol{x}) \\ p_2(\boldsymbol{x}) \\ p_3(\boldsymbol{x}) \end{pmatrix} = \begin{pmatrix} u^L(\boldsymbol{x}) \\ u^H(\boldsymbol{x}) \\ 1 \end{pmatrix} \tag{3}$$

By solving this liner system in Equation (3) using Cramer's rule, and by recalling that the determinants correspond to the signed areas A_1, A_2, and A_3, as illustrated in Fig. 2, we get,

$$p_1 = {}^{A_1}\!/_{A}\ ,\ p_2 = {}^{A_2}\!/_{A}\ ,\ p_3 = {}^{A_3}\!/_{A}, \tag{4}$$

where A is the signed area of triangle $m_1m_2m_3$.

Indeed, p_1, p_2, p_3 sum to 1 and the three vertices have barycentric coordinates, $m_1(1,0,0)$, $m_2(0,1,0)$, and $m_3(0,0,1)$. Also, points inside the triangle have positive p_i; and points outside the triangle have at least one negative coordinate.

In CTC, we set three base materials to air (m_1), soft tissue (m_2), and iodine-tagged fecal residual (m_3). Thus, each voxel may be decomposed into a mixture of these three materials.

B. Adaptive Classification

CT values of air and soft tissue at different energies can be calculated using NIST XCOM program [11] with the input of manufacturer supplied effective photon energies of the scanner, such as 51.3 keV at 80 kVp and 91.0 keV at 140 kVp for SOMATON Definition Flash (Siemens Healthcare, Germany).

However, there is a large variability in iodine-tagged fecal residue in the DE-CTC data due to the different tagging levels at different parts of the colon. To account for the local tagging level of iodine, we compute the local CT value $(u^L_{\text{tagging}}, u^H_{\text{tagging}})$ of iodine-tagged fecal residuals using a 3D bounding box automatically defined in an isolated tagged region.

The bounding box is calculated in 140 kVp images, which has lower noise than that of 80 kVp. To separate individual iodine-tagged regions in the colon, we apply a morphological opening operator for the removal of weak connection in the tagging components. Then, a minimum bounding box B_i is calculated for each separated region V_i by defining the box to be:

$$\begin{aligned} \min\{x_i\} \le x \le \max\{x_i\} \\ \min\{y_i\} \le y \le \max\{y_i\} \\ \min\{z_i\} \le z \le \max\{z_i\} \end{aligned} \tag{5}$$

where each voxel $v_i(x_i, y_i, z_i) \in V_i$.

Within each bounding box B_i, a homogeneous tagging mask is calculated under the condition that the gradient magnitude has less than a pre-defined threshold, such as

$$u(\boldsymbol{x}) > 200 \text{ HU and } |\nabla u(\boldsymbol{x})| < 300.$$

In each bounding box B_i, the mean CT values $(u^L_{\text{tagging}}, u^H_{\text{tagging}})$ of the iodine-tagged region within the homogeneous tagging mask are calculated as the local CT value of the iodine-tagged material.

Thus, for each voxel v_i, the local $(u^L_{\text{tagging}}, u^H_{\text{tagging}})$ of the nearest bounding box B_i were employed in Equation (3) under the following conditions:

- if $v_i \in B_i$, then $(u^L_{\text{tagging}}, u^H_{\text{tagging}})$ of B_i was selected.
- if $v_i \notin B_i$ then the $(u^L_{\text{tagging}}, u^H_{\text{tagging}})$ of the B_i that has the nearest distance was selected. The distance between v_i and B_i was calculated based on the surface of the bounding box.

C. Virtual Tagging

Virtual tagging (VT) is a means of marking the entire colonic lumen on DE-CTC images, including air and tagged fecal materials, as well as their mixture in the colon, to

differentiate soft tissue from air-tagging mixture caused by the PVE, and thus reducing the cleansing artifacts.

Suppose that (p_1, p_2, p_3) is the mixture vector at voxel v_i. Virtual tagging recalculates the CT value of each voxel $u^{VT}(\boldsymbol{x})$ using Equation (6) with a pre-defined CT values of u^{VT}_{air} for air, u^{VT}_{ST} for soft tissue, and u^{VT}_{tagging} for tagged material. For the purpose of tagging the entire colonic lumen, we set both air and tagged materials having higher CT values, whereas soft tissue has CT values of zero.

$$u^{VT}(\boldsymbol{x}) = p_{\text{air}}(\boldsymbol{x}) \cdot u^{VT}_{\text{air}} + p_{\text{ST}}(\boldsymbol{x}) \cdot u^{VT}_{\text{ST}} + p_{\text{tagging}}(\boldsymbol{x}) \cdot u^{VT}_{\text{tagging}} \qquad (6)$$

where we set u^{VT}_{air} = 600 HU, u^{VT}_{ST}=0 HU, and u^{VT}_{air} = 500 HU.

Fig. 3(c) displays a VT image of Fig. 3(a) and (b). We observed that the AT-boundary was virtually tagged and differentiated clearly from the soft-tissue structures in the VT image of Fig. 3(c). In addition, we observed that the air bubbles submerged in the tagged region were virtually tagged and the tagging inhomogeneity was significantly reduced in the VT image.

D. Hessian Response of VT Image

We applied the *structure-analysis* EC scheme (SA-Cleansing) [12] for cleansing the virtually-tagged colon lumen. The SA-Cleansing scheme uses the local morphologic information to classify the submerged soft-tissue structures while removing the tagged materials. Specifically, in the VT images, we use the eigenvalue signatures of a Hessian matrix to enhance the submerged fold-like and polyp-like structures, whereas other structures were de-enhanced and thus may be subtracted from the CTC images.

Morphologically, folds and polyps submerged in the tagged regions present rut-like (concave ridge) and cup-like (concave cap) shapes because the surrounding tagged materials have higher CT values than do those for soft-tissue structures. Based on the eigenvalue signatures that are characteristic of folds and polyp structures, a *cup-enhancement function* (F_{cup}) and a *rut-enhancement function* (F_{rut}) were formulated [12], so that their product had a high response from submerged polyps and folds. In Fig. 3(d), we demonstrated the Hessian response of Fig. 3(c). We observed that Hessian response filed could preserve well the submerged folds and polyps.

E. DE-EC Scheme

We have developed a DE-EC scheme for fecal-tagging DE-CTC that was performed in a 3D manner. The DE-EC scheme consists of the following five steps: (1) initial segmentation of the colon [12], (2) virtual tagging of the colon using three-material decomposition, (3) computation of Hessian response field in virtual-tagged images, (4) segmentation of tagged regions based on the level set method, and (5) replacement of the tagged regions that are segmented in step (4) with air, followed by reconstruction of the colonic wall submerged in tagged regions.

To segment the tagged materials precisely and subsequently remove (cleanse) them from the colonic lumen, we employed a level-set method combined with the gradient field (G) and the Hessian response field (H) from the VT images. The level-set front is initialized by the classified tagged regions, and it is evolved by use of the partial differential equation shown below:

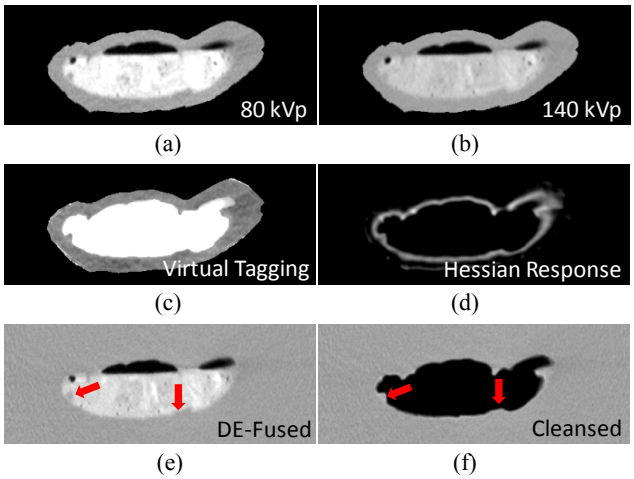

Fig. 3. Illustration of virtual tagging and electronic cleansing of a pig colon in DE-CTC study. (a, b) A pair of transverse DE-CTC images at (a) low energy of 80 kVp and at (b) high energy of 140 kVp. (c) Virtual-tagging image for (a) and (b). Both the air-tagging mixture and the air bubbles submerged in the tagged fecal materials are virtually well-tagged. (d) Hessian-response image of (c). (e) Fused image of (a) and (b), in which 30% of the 80 kVp images are mixed with 70% of 140 kVp images. (f) The cleansed image of (e) after the application of the DE-EC scheme. The red arrows pointed at two polyps submerged in the tagged materials before (e) and after (f) the application of the DE-EC scheme.

$$\partial\Phi/\partial t = -(F_H(\boldsymbol{x}) + F_G(\boldsymbol{x}) + F_S)|\nabla\Phi| \,. \qquad (7)$$

Here, $\boldsymbol{x}$ is the point on the level-set front. F is a speed function, for which we employ a conventional threshold speed function [17]. This evolution equation has two speed functions from images: the speed function of image gradients, $F_G(\boldsymbol{x})$, and the speed function of the Hessian response field, $F_H(\boldsymbol{x})$. These speed functions are balanced with F_S, which is a smoothing term of the shape of the level-set front that is proportional to the mean curvature flow, $F_S \propto \nabla(\nabla\Phi/|\nabla\Phi|)$, ensuring the numerical stability of the forward-in-time, centered-in-space solution of the partial differential equation [13]. With use of these speed functions, the level-set front becomes sensitive to soft-tissue structures, whereas it is insensitive to the tagged regions. Thus, tagged regions are segmented and removed with the air-tagging boundaries, whereas the soft-tissue structures are preserved. Fig. 3(f) demonstrates the effectiveness of the DE-EC scheme in cleansing the air-tagging mixture and inhomogeneous tagging in Fig. 3(e).

III. Results

Twenty-three patients underwent a 24-hour bowel preparation with a low-fiber, low-residue diet, oral administration of 50 ml non-ionic iodine (300 mg/ml concentration of Omnipaque iohexol, GE Healthcare, Milwaukee, WI). DE-CT scanning (SOMATON Definition, Siemens Healthcare, Germany) was performed at tube voltages of 140 kVp and 80 kVp with automatic dose exposure control module (CARE Dose 4D) in both supine and prone positions. For both supine and prone scanning, we used the soft tissue reconstruction kernel (B30f), and a 0.625

mm slice reconstruction interval. In total, there were 48 pathology-confirmed polyps ≥6mm, in which 7 polyps were submerged in the tagged materials.

After the application of proposed DE-EC scheme, initial evaluation showed that the EC artifacts were significantly reduced. We observed 0 to 1 minor EC artifacts per case compared to the 5 to 6 significant EC artifacts in previous single energy EC methods. In addition, all submerged polyps were clearly visualized without EC artifacts.

Fig. 4 demonstrates comparisons between our DE-EC scheme and two single-energy EC packages: a commercial EC package and our previously developed SA-Cleansing. Both single-energy EC packages were performed on the fused DE-CTC images. Fig. 4(a) and (b) were generated by the commercial EC package. Here, we observe that both images suffered from EC artifacts, such as broken folds, deformed polyps (marked by the viewing box), false fistula, as well as false patch. Fig. 4(c) and (d) were created by the SA-cleansing scheme. EC artifacts were reduced significantly by use of morphological analysis. However, a thin layer cause by PVE was missed and displayed. Fig. 4(e) and (f) were generated by the DE-EC scheme, in which both images were free from any types of EC artifacts.

IV. Conclusions

In our study, we observed that the virtual tagging of colon using DE-CTC images provides us an effective means to remove EC artifacts caused by the air-tagging mixture and tagging inhomogeneity. Initial evaluation of the results based on the pig colon and clinical cases showed that our DE-EC method can effectively differentiate soft tissue from air-tagged mixtures; thus, it provides an artifact-free visualization of the colonic lumen for fecal-tagging CTC. Our new method is potentially useful for efficient reduction of the EC artifacts, leading to cleansed CTC images of diagnostic quality.

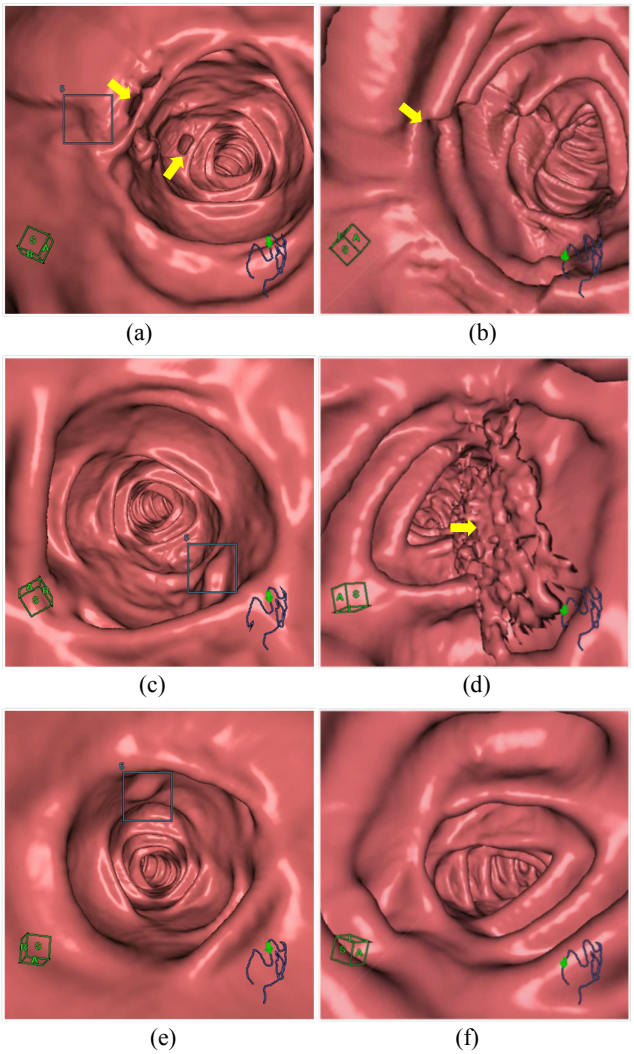

Fig. 4. Comparisons between the DE-EC scheme and two conventional single-energy EC packages. (a, b) Cleansed images generated by a commercial EC package: We observed severe EC artifacts: broken folds, false fistula, and false patch (yellow arrows), as well as the shrunken polyp (viewing box). (c, d) Cleansed images generated by SA-Cleansing scheme: The polyp is well preserved (viewing box), whereas parts of the air-tagging mixture were not cleansed (yellow arrow). (e,f) Cleansed images generated by the DE-EC scheme: The colon is well cleansed and free from any EC artifacts. The polyp is also well preserved.

References

[1] Cai W, Yoshida H, Zalis ME, Näppi J. Delineation of tagged region by use of local iso-surface roughness in electronic cleansing for CT colonography. Proc SPIE Medical Imaging: Computer-Aided Diagnosis 2007; 6514 1-9.

[2] Wang Z, Liang Z, Li X, et al. An improved electronic colon cleansing method for detection of colonic polyps by virtual colonoscopy. IEEE Transactions on Bio-medical Engineering 2006; 53:1635-46.

[3] Bazalova M, Carrier J, Beaulieu L, Verhaegen F. Dual-energy CT-based material extraction for tissue segmentation in Monte Carlo dose calculations. Phys Med Biol 2008; 53:2439-2456.

[4] Johnson TR, Krauss B, Sedlmair M, et al. Material differentiation by dual energy CT: initial experience. Eur Radiol 2007; 17:1510-7.

[5] Roessl E, Proksa R. K-edge imaging in x-ray computed tomography using multi-bin photon counting detectors. Phys Med Biol 2007; 52:4679-4696.

[6] Schlomka JP, Roessl E, Dorscheid R, et al. Experimental feasibility of multi-energy photon-counting K-edge imaging in pre-clinical computed tomography. Phys Med Biol 2008; 53:4031-4047.

[7] Zalis ME, Perumpillichira JJ, Magee C, Kohlberg G, Hahn PF. Tagging-based, electronically cleansed CT colonography: evaluation of patient comfort and image readability. Radiology 2006; 239:149-59.

[8] Raz Carmi, Galit Kafri, Liran Goshen, et al. A unique noncathartic CT colonography approach by using two-layer dual-energy MDCT and a special algorithmic colon cleansing method. IEEE 2008 NSS-MIC conference 2008; M10:132.

[9] Cai W, Liu b, Yoshida H. Dual-energy electronic cleansing scheme for non-cathartic CT Colonography: a phantom study. Radiological Society of North America scientific assembly and annual meeting program 2009; 466-466-467.

[10] Cai W, Yoshida H, Kim SH, Lee J. Dual-energy electronic cleansing for non-cathartic fecal-tagging CT colonography based on dual-energy index. 97th Scientific Assembly and Annual Meeting of RSNA 2011;

[11] Berger M, Hubbell J, Seltzer S, et al. XCOM: Photon Cross Sections Database (version 3.1). Radiation and Biomolecular Physics Division, PML, National Institute of Standard and Technology, Last Updated: Dec. 09, 2011; http://www.nist.gov/pml/data/xcom/.

[12] Cai W, Zalis ME, Näppi J, Harris GJ, Yoshida H. Structure-analysis method for electronic cleansing in cathartic and noncathartic CT colonography. Med Phys 2008; 35:3259-77.

[13] Ho S, Bullitt E, Gerig G. Level set evolution with region competition: automatic 3-D segmentation of brain tumors. Proceedings of 16th International Conference on Pattern Recognition 2002; 532-535.